

Comparison of the quality of $\text{Bi}_{12}\text{GeO}_{20}$ crystals grown by the conventional and low-temperature-gradient Czochralski techniques

V.N.Shlegel, D.S.Pantsurkin

A. Nikolaev Institute of Inorganic Chemistry, Siberian Branch of the Russian Academy of Sciences, 3 Acad. Lavrentiev Ave., 630090 Novosibirsk, Russia

Received 27 May, 2010

Comparison of the quality of $\text{Bi}_{12}\text{GeO}_{20}$ (BGO) crystals grown by the conventional and low-temperature-gradient Czochralski techniques is carried out. The crystals were grown along the $\langle 111 \rangle$ direction under close process parameters except for thermal gradients, from the same initial components. Dependencies of morphogenesis and crystal quality on growing conditions were described. Comparison of macro-defects was carried out, the density of dislocations was evaluated, and the homogeneity of optical density was surveyed for the crystals grown under the conditions of low and high thermal gradients.

Проведено сравнение качества кристаллов $\text{Bi}_{12}\text{GeO}_{20}$ (BGO), выращенных традиционным (Cz) и низкоградиентным (LTG Cz) методом Чохральского. Кристаллы выращивались в направлении $\langle 111 \rangle$ при близких параметрах процесса, за исключением температурных градиентов, из одних и тех же исходных компонентов. Описаны зависимости формообразования и качества кристаллов от условий выращивания. Проведено сравнение макродефектов, оценена плотность дислокаций и однородность оптической плотности кристаллов, полученных в условиях низких и высоких градиентов.

1. Introduction

Crystals with sillenite structure are still of interest due to a combination of practically valuable properties: piezoelectric, electro- and magneto-optical, optical activity, photoconductivity and photorefraction. Sillenite crystals are used in piezosensors, filters and delay circuits for electromagnetic signals, electro- and magneto-optical field-strength meters, space-time modulators etc.

The main growth method of BGO is the conventional Czochralski (Cz) technique [2]. One of the major problems for growing the compounds with sillenite structure under the conditions of high thermal gradient is to obtain crystals with high optical homogeneity [3–12]. Two most characteristic types of "optical" defects in these crystals are dis-

tinguished: inclusion of extraneous phases and the presence of regions with increased optical density in the volume of crystal. The existence of the regions with increased optical density in crystals with sillenite structure may be exhibited as the growth bands and the so-called growth column [2]. In the opinion of the authors of [8–10, 13], the appearance of a growth column and the effect of selective decoration in the form of a three-blade propeller during growing along $\langle 111 \rangle$ direction are due to the anisotropy of growth rates and differences in the coefficients of distribution of "photochromic" admixtures for polar $\{110\}$ and non-polar $\{100\}$ faces present at the crystallization front. The appearance of the regions with increased optical density also may be a consequence of the coexistence of the normal

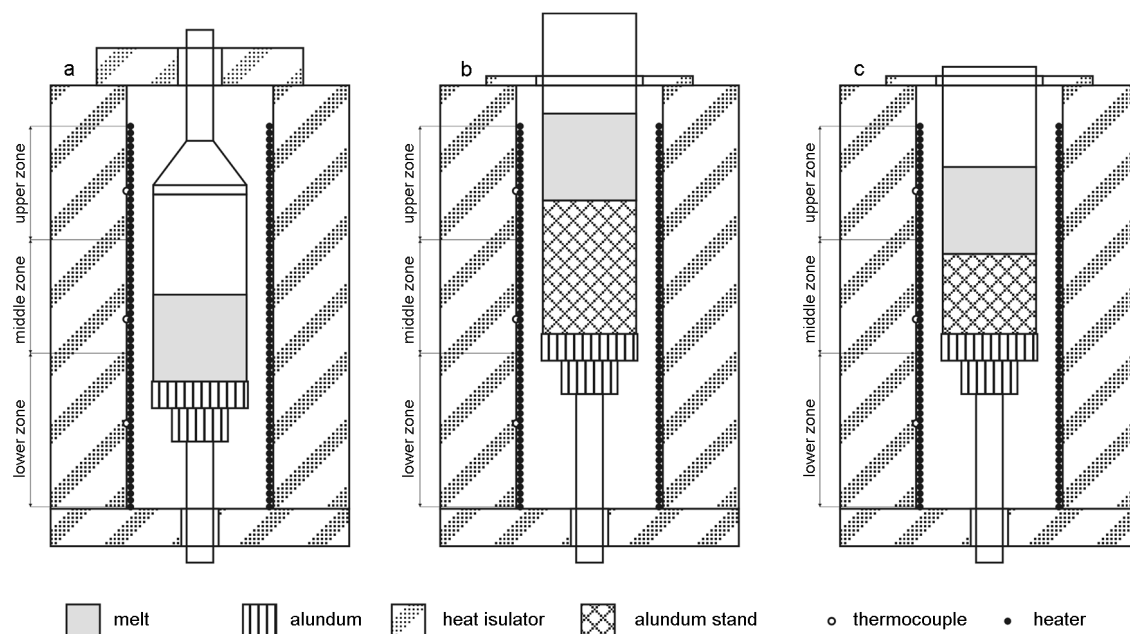


Fig. 1. Schematics of furnace of HX620 crystal growth setup: a — original setup, b, c — remodeled setups.

and layer-by-layer growth mechanisms at the crystallization front [14]. The sources of optical heterogeneity in the case of the layer-by-layer crystal growth mechanism, as the authors of [13] suppose, are the possibility of deviation of the crystal composition from the stoichiometric one within the homogeneity region and variation of the concentration of admixtures during temperature fluctuations. According to [15], the reason of the variation of the optical density of sillenite crystals is the possibility for the conditions leading to the formation of metastable phases in these systems. According to [2], the density of dislocations in BGO single crystals varies from $1 \cdot 10^2 \text{ cm}^{-2}$ in the defect-free region to $5 \cdot 10^4 \text{ cm}^{-2}$ in the region containing inclusions.

Previously, we carried out the work [16, 17] aimed at growing BGO crystals using the Low Temperature Gradient Cz technique and studied the quality of the grown crystals by means of interferometry and X-ray topography. However, no direct comparison between the crystals grown under radically different conditions with respect to thermal gradients was made. The present work aimed at the growth of BGO crystals by means of Cz and LTG Cz from identical initial components under identical growth parameters, and with comparison of the obtained crystals.

2. Experimental details

We described BGO crystal growth using the LTG Cz technique in detail previously [16, 17]. In the present work, growing BGO under the conditions of the high thermal gradients, we used similar growth parameters and the setup (HX620M). The crystals were grown from a platinum crucible 70 mm in diameter and 150 mm high, placed in a three-zone furnace with independent temperature control contours. In the usual configuration, when the crystals are grown under low thermal gradients, the crucible with the cap is placed in the three-zone furnace equipped with thick heat-insulating layers from above and from beneath (Fig. 1a). An increase in thermal gradient was achieved due to changes in the design of separate units of the crystallization cell of the growth setup without changing the furnace in whole. The upper heat-insulating layer was made thinner. Platinum cap, that had been playing the part of thermal screen and diffusion barrier, was removed. By increasing the height of the support, the crucible with the melt was lifted relative to heaters in the furnace. The melt level was even higher than the end of the upper heater as shown in Fig. 1b. Such a configuration provided strong heat sink from the open surface of the melt. The growing crystal was inside the region of high thermal gradients. Temperature difference between the heater and the crucible was several de-

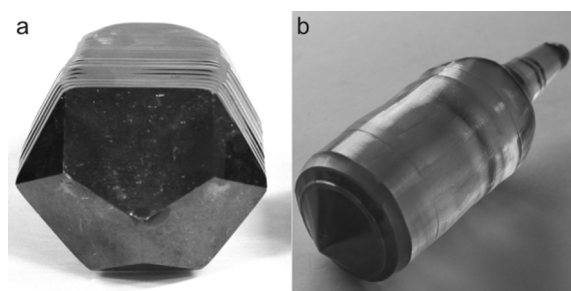


Fig. 2. BGO crystals grown by: a — LTG Cz technique, b — Cz technique.

grees in the growth cell arranged as shown in Fig. 1a, while in the case shown in Fig. 1b, c this difference reaches 250°C . Power required to keep the charged mass melted is 1.5–2 times lower in the case shown in Fig. 1a than in a similar case for the open system (Fig. 1b, c).

Evidently, the axial and radial thermal gradients for the modification of the heat unit presented in Fig. 1b, c are substantially higher than those occurring in the original design of the heat unit. A stoichiometric mixture of Bi_2O_3 and GeO_2 was used as the furnace charge. The procedure of melt preparation was the same as that described in [16]. In both cases, melting and homogenization proceeded without any specific features. An essential difference was noticeable evaporation of the melt under the conditions of the high thermal gradient. Exposure of the melt at a temperature of 945°C for 24 h caused a mass loss from 5 to 30 g (0.25–1.5 mass.% of the charge mass).

Seeding was carried out using a BGO seed oriented along the $\langle 111 \rangle$ direction. Rotation frequency was constant in all the processes and equal to 20 r.p.m, crystallization rate was varied from 0.5 to 3 mm/h.

Crystals 30–50 mm in diameter, with the length of 70 to 100 mm, were obtained using both growing techniques. Growth regularities and the appearance of BGO crystals obtained under the conditions of low gradients were described in detail in [16]; a typical crystal shape is presented in Fig. 2a. The crystals grown using the Cz technique were shaped as a cylinder with crystallization front as a rotation figure, most frequently as a cone (Fig. 2b). With definite process parameters, crystals with weakly convex, almost flat crystallization front were obtained. As expected, unlike for the LTG Cz technique, under the growth conditions with the high thermal gradient

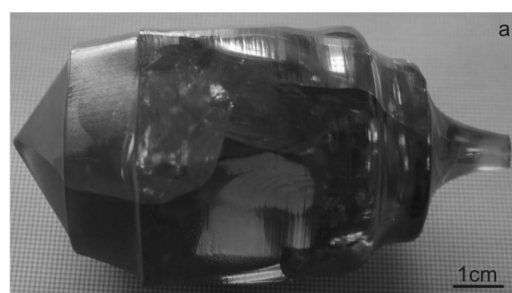


Fig. 3. BGO crystals grown using: a — setup Fig. 1b, b — setup Fig. 1c.

we did not encounter such complications as the formation of a parasitic crystal at the bottom and/or wall of the crucible and a drift of the crystal off the rotation axis. However, in the case of the high thermal gradient, more essential problems in obtaining the crystals of satisfactory quality appeared.

First of all, growth under the high thermal gradients resulted in the formation of strained crystals. The BGO crystals grown with the heat unit design shown in Fig. 1b had a diameter not more than 30 mm. The crystals of larger diameter were cracking at the stage of annealing even with annealing rate of $20^{\circ}/\text{h}$ (Fig. 3a). With the heat unit design providing less sharp thermal gradients (Fig. 1c), at the crystallization rate of 0.5–1 mm/h, we succeeded in obtaining relatively unstrained crystals with the diameter up to 50 mm (Fig. 3b). At the crystallization rate of 1.5 mm/h, the crystals cracked during mechanical treatment rather frequently, while at the rate of 3 mm/h the crystals cracked as early as at the stage of annealing.

The defect structure of the crystals was studied by means of selective chemical etching and interferometry. To study the quality of BGO crystals grown under the low gradient conditions, we used the material obtained through crystal growth with layer-by-layer growth mechanism in the direct vicinity to the front, in the presence of clearly formed faces, so that one could be

Table. Behavior of etchants based on HCl and HNO₃ on BGO surface.

Etchant composition	Components volume ratio	Etching conditions		BGO samples orientation	Etching behavior
		Time, min	Temperature, °C		
HCl(5M)	–	<1	20–25	<100>	<110>
HCl(5M):H ₂ O ₂ (28 %)	1:1	<1	20–25	<100>	<110>, <111>
HCl(5M):NH ₄ Cl(5M)	1:2, 1:3, 1:4	7–25	20–20	<111>	Nonselective dissolution of surface, formation of not faceted etching pits
HCl(5M):C ₃ H ₅ (OH) ₃	2:3	30–60	20–25	<100>, <110>, <111>	Surface polishing
		90		<111>	Surface polishing, formation of faceted etching pits
HNO ₃ (5M)	–	10–30	20–25	<110>	Surface unchanged
		30	40–45		Surface polishing
		>30			Nonselective dissolution of surface
HNO ₃ (5M):H ₂ O ₂ (28 %)	1:1	10–30	20–25	<110>	Surface polishing
		30	40–45		Surface polishing, nonselective dissolution of surface
		>30			Nonselective dissolution of surface
HNO ₃ (5M):NH ₄ NO ₃ (5M)	1:2, 1:3, 1:4	10–30	20–25	<110>	Surface unchanged
		30	40–45		Surface polishing
		>30			
HNO ₃ (5M):AcOH(ice)	1:1, 1:2	30	45–55	<110>	Nonselective dissolution of surface, formation of faceted etching pits
		60		<111>	
	2:1	30	<110>	Formation of faceted etching pits	
		60	<111>		

sure that we examine the crystal part grown layer by layer. Orientation of the samples was performed on the basis of their habit. In the case of the crystals grown under the high gradient, cuts perpendicular to the growth direction were used. Deviation from the crystallographic direction could be 2–3°. Examination by means of selective chemical etching was carried out using the plates 2–2.5 mm thick; interferometric studies were performed with crystal sections 10–15 mm thick. Deviation from parallelism of the opposite planes of the sample did not exceed 30". The samples were smoothed and polished mechanically, then chemically with the solutions of hydrochloric acid in glycerol (Table).

Samples were etched with the solutions based on hydrochloric and nitric acids; the

efficiency of these solutions towards BGO crystals is well studied. The results of the interaction of different etchants with sample surface are presented in Table. The reliability of the results of selective etching was confirmed with the help of X-ray topography. The data obtained in the investigation of BGO by means of X-ray topography were reported in [16]. According to the data of selective chemical etching, the density of dislocations in crystal grown at low thermal gradients in the layer-by-layer mode did not exceed 10 cm². During BGO etching, only sole dislocations were exhibited on the sample surface (Fig. 4a). The density of dislocations in the crystals grown under the high gradients of temperature was 10³–10⁴ cm² (Fig. 4b, c).

Relative optical homogeneity of samples was evaluated using Jamin interferometer.

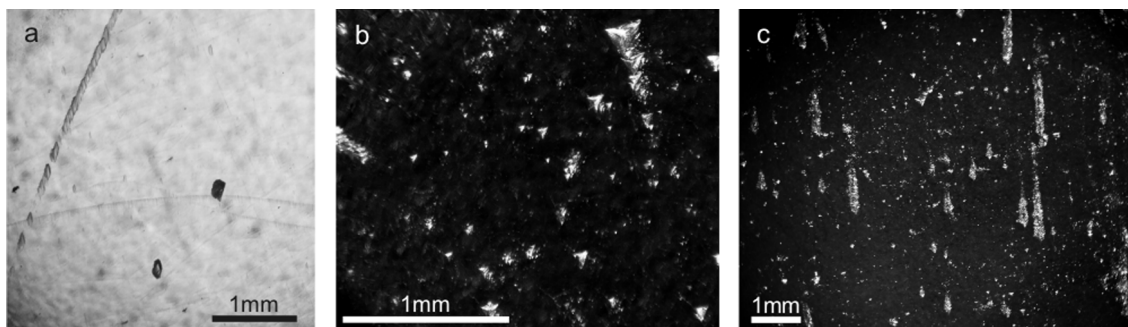


Fig. 4. Etching pits on BGO surface: a — BGO grown by LTG Cz, sample oriented along $\langle 110 \rangle$ direction; b, c — BGO grown by Cz, samples oriented along $\langle 111 \rangle$ direction. Etchant — $\text{HNO}_3:\text{AcOH}/2:1$, 50°C , 30 min.

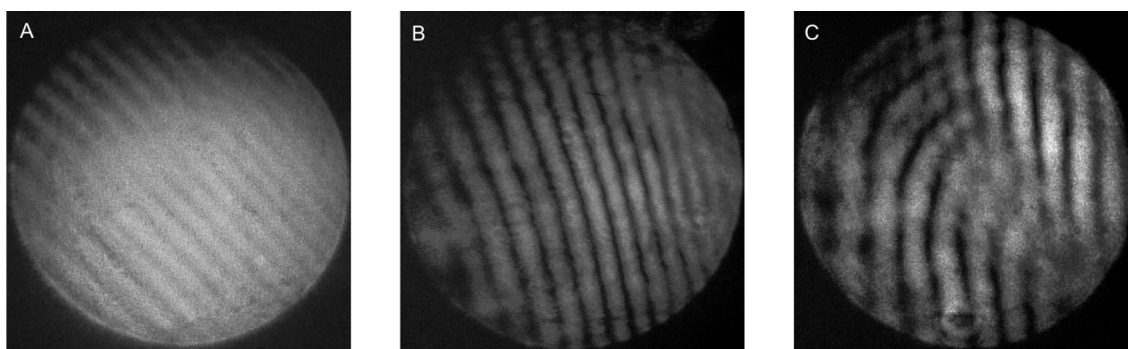


Fig. 5. Interference images of $\text{Bi}_{12}\text{GeO}_{20}$ samples: a — typical interference image of BGO grown by LTG Cz; b, c — interference image of BGO grown by Cz.

The scheme of the instrument, measurement procedure and the data of measurements of the optical homogeneity of BGO crystals grown by means of LTG Cz were described in [17]. In the investigation of BGO samples grown under the conditions of low thermal gradient and containing no inclusions, the interference images remained stable, that is, the width and shape of interference bands did not change, even in the crystal regions formed by the vertex and face regions of the crystallization front. An example of a typical interference image of a BGO sample is shown in Fig. 5a. In the case of BGO Cz crystals, nonhomogeneity of bands was observed in the interference images: broadening between the bands and their hooking (Fig. 5b). Regions with substantial distortions of the behaviour of interference bands were detected; this is shown in Fig. 5c.

3. Discussion of results

For the first time, the growth of BGO crystals was carried out according to the Cz and LTG Cz techniques using identical initial components, at maximally similar growth parameters. A comparison of the density of dislocations and the homogeneity of optical density of BGO crystals grown

under the conditions of low and high thermal gradients was carried out. It was established that the density of dislocations in BGO LTG Cz crystals is not more than 10 cm^{-2} , while for BGO Cz crystals this value is 2–3 orders of magnitude larger. The comparison of the homogeneity of optical density showed that the nonhomogeneity of the crystals grown using the low-temperature-gradient Czochralski technique did not exceed 10^{-3} . In BGO Cz crystals, this value was not less than $3 \cdot 10^{-3}$. The BGO crystals grown under the high thermal gradients were found to contain the regions of sharp changes of the optical density, which may be an evidence of the presence of block boundaries and the regions of strain concentration in the crystals.

Technological problems were encountered when growing BGO crystals under the high thermal gradients. The crystals are prone to splitting, especially at the stages of the crystal detachment from the melt and annealing. Substantial evaporation of the melt, namely its low-melting component Bi_2O_3 , caused the loss of the charged material and disturbed the stoichiometry of the melt, which also could have a negative effect on the quality of the crystals.

4. Conclusions

Radical decrease of thermal gradients during the growth of BGO crystals undoubtedly causes improvement of their quality, namely improvement of the homogeneity of optical density and a decrease in the density of dislocations.

References

1. A.A.Pavlyuk, Ya.V.Vasiliev, F.A.Kuznetsov, in: Proc. of APSAM-92, Shanghai, China (1992), p.164.
2. Yu.F.Kargin, V.I.Burkov, A.A.Mar'in, A.V.Egorisheva, $\text{Bi}_{12}\text{M}_x\text{O}_{20\pm\delta}$ Crystals with Sillenite Structure. Synthesis, Structure, Properties, Kigic, Moscow (2004) [in Russian].
3. A.A.Ballman, *J. Cryst. Growth*, **1**, 37 (1967).
4. A.I.Safonov, S.A.Barishev, T.I.Nikiforova, *Kristallografiya*, **13**, 914 (1968).
5. A.I.Safonov, S.A.Barishev, T.I.Nikiforova, *Kristallografiya*, **14**, 152 (1969).
6. T.M.Safronov, V.N.Batog, Yu.I.Krasilov, *Neorg. Mat.*, **6**, 284 (1970).
7. A.T.Sobolev, Yu.L.Kopilov, V.B.Kravchenko, *Kristallografiya*, **23**, 174 (1978).
8. Yu.S.Kuz'minov, M.G.Lifsits, V.D.Sal'nikov, *Kristallografiya*, **14**, 363 (1969).
9. J.C.Brice, T.M.Bruton, O.F.Hill, *J. Cryst. Growth*, **24/25**, 429 (1974).
10. A.R.Tanguay, S.Mroczkowski, R.C.Barker, *J. Cryst. Growth*, **42**, 431 (1977).
11. F.Smet, W.J.P.Van Enckevort, *J. Cryst. Growth*, **100**, 417 (1990).
12. O.N.Budenkova, M.G.Vasilev, E.N.Bystrova, *J. Cryst. Growth*, **266**, 103 (2004).
13. B.Steiner, U.Laor, M.Kuriyama, *J. Cryst. Growth*, **87**, 79 (1988).
14. Yu.A.Borovlev, N.V.Ivannikova, V.N.Shlegel, *J. Cryst. Growth*, **229**, 305 (2001).
15. V.P.Jereb, V.M.Skorikov, *Neorg. Mat.*, **39**, 11365 (2003).
16. V.N.Shlegel, D.S.Pantsurkin, *Crystallography Reports*, **54**, 1261 (2009).
17. V.N.Shlegel, D.S.Pantsurkin, *Crystallography Reports*, (2010) (in print)

Порівняння якості кристалів $\text{Bi}_{12}\text{GeO}_{20}$, вирощених традиційним і низькоградієнтним методом Чохральського

В.Н. Шлегель, Д.С. Панцуркін

Проведено порівняння якості кристалів $\text{Bi}_{12}\text{GeO}_{20}$ (BGO), вирощених традиційним та низькоградієнтним методами Чохральського. Кристали вирощувалися у напрямку $\langle 111 \rangle$ при близьких параметрах процесу, за виключенням температурних градієнтів, з одних і тих ісходних компонентів. Описано залежності формотворення і якості кристалів від умов вирощування. Проведено порівняння макродефектів, оцінено щільність дислокацій та однорідність оптичної щільності кристалів, що отримані в умовах низьких та високих градієнтів.